**Distribution Agreement**

In presenting this thesis as a partial fulfillment of the requirements for a degree from Emory University, I hereby grant to Emory University and its agents the non-exclusive license to archive, make accessible, and display my thesis in whole or in part in all forms of media, now or hereafter now, including display on the World Wide Web. I understand that I may select some access restrictions as part of the online submission of this thesis. I retain all ownership rights to the copyright of the thesis. I also retain the right to use in future works (such as articles or books) all or part of this thesis.

Liz Enyenihi April 12, 2020

# Functional Analysis of RNA Exosome Mutants Linked to Disease Using a Budding Yeast Model

by

Liz Enyenihi

Anita H. Corbett and Milo B. Fasken
Advisers

Chemistry

Anita H. Corbett and Milo B. Fasken
Advisers

David Lynn
Committee Member

Jen Heemstra
Committee Member

2020

# Functional Analysis of RNA Exosome Mutants Linked to Disease Using a Budding Yeast Model

By

Liz Enyenihi

Anita H. Corbett and Milo B. Fasken

Advisers

An abstract of
a thesis submitted to the Faculty of Emory College of Arts and Sciences
of Emory University in partial fulfillment
of the requirements of the degree of
Bachelor of Science with Honors

Chemistry

2020

Abstract

Functional Analysis of RNA Exosome Mutants

Linked to Disease Using a Budding Yeast Model

By Liz Enyenihi

Regulation of gene expression at many levels is critical to control the fate and function of all cell types. While transcriptional regulation is important, RNA processing enzymes also play a crucial role in regulating gene expression. The RNA exosome is an evolutionarily conserved, multi-subunit complex that both processes and degrades many classes of RNA. Mutations in genes encoding subunits of the RNA exosome cause a number of significant neurological diseases that lead to drastically shortened lifespans. My research investigates how amino acid substitutions in a structural subunit of the RNA exosome, EXOSC2, affect overall RNA exosome function, with a particular focus on the amino acid substitutions that have been linked to a novel neurodegenerative syndrome in humans. As part of a broader analysis of RNA exosome models that I contributed to, I generated a budding yeast model to assess the functional consequences of missense mutations in *EXOSC2* that are linked to disease. Using this model, I conducted experiments to assess the growth, steady state RNA levels, protein levels, and potential cofactor interactions in budding yeast. I found that the yeast ortholog of the EXOSC2 G30V variant was lethal while the yeast ortholog of the EXOSC2 G198D variant caused a temperature sensitive growth defect, reduction in protein level, accumulation of some known RNA exosome substrate transcripts. Furthermore, I exploited yeast genetics approaches to identify genetic interactions with the nonessential RNA exosome cofactors Mpp6 and Rrp47. Taken together, my studies provide insight into how specific amino acid changes could impact RNA exosome function and contribute to disease pathology.

# Functional Analysis of RNA Exosome Mutants Linked to Disease Using a Budding Yeast Model

By

Liz Enyenihi

Anita H. Corbett and Milo B. Fasken

Advisers

A thesis submitted to the Faculty of Emory College of Arts and Sciences
of Emory University in partial fulfillment
of the requirements of the degree of
Bachelor of Science with Honors

Chemistry

2020

Acknowledgements

I owe many thanks to all the members of the Corbett lab who have given me invaluable guidance and support as I worked on this project. I would like to especially thank Dr. Milo Fasken who patiently trained me for the past four years. Thank you for painstakingly showing me how to do things correctly and for imparting so much scientific knowledge to me. Your advice and reassurance have been incredibly helpful. I could not have completed this project without all of your support and wisdom.

I would also like to thank Dr. Anita Corbett for giving me the amazing opportunity to work in her research lab. Despite starting as a first-year student with little background biological knowledge, she saw my potential and has encouraged me so much on my academic journey. I appreciate your continuous support and advice, and I hope to provide similar mentorship to students in the future. My experience in this lab has inspired me to pursue becoming a professor, and I look forward to a scientific career full of new discoveries.

## TABLE OF CONTENTS

# INTRODUCTION

Although all eukaryotic cells within an organism contain the same DNA blueprint, selective gene expression allows these cells to look and function differently. A critical step in this control of gene expression occurs when the RNA message is processed and regulated. The RNA exosome, which is an evolutionarily conserved, multi-subunit complex, is a key component of RNA processing and quality control that degrades and/or processes messenger RNA, small nuclear RNA, ribosomal RNA, transfer RNA, and other unstable transcripts (Fasken et al., 2020).

The RNA exosome executes different functions in the nucleus and cytoplasm. In the nucleus, the RNA exosome processes noncoding RNAs (ncRNAs) and functions in nuclear surveillance pathways by degrading improperly processed RNAs and cryptic transcripts that result from pervasive transcription (Kilchert et al., 2016). Additionally, a critical function of the nuclear RNA exosome is to produce mature, properly processed ribosomal RNA (rRNA) (Allmang et al., 1999) as well as small ncRNAs, including small nuclear RNAs (snRNAs), small nucleolar RNAs (snoRNAs), transfer RNAs (tRNAs) and other non-coding RNAs, such as cryptic unstable transcripts (CUTs) and *TLC1*, the telomerase RNA in budding yeast. The nuclear RNA exosome has also been implicated in transcription termination, maintenance of genome integrity via resolving RNA-DNA hybrids, and antibody class switching (Kilchert et al., 2016). The cytoplasmic RNA exosome degrades aberrant messenger RNA (mRNA) transcripts and nonstop mRNAs in mRNA surveillance pathways and also functions in nonsense-mediated mRNA degradation (Schaeffer et al., 2010).

The specificity of the RNA exosome for different RNA substrates is thought to be conferred by several nuclear and cytoplasmic cofactors (Zinder and Lima, 2017). The nuclear exosome cofactor, Mpp6, is an RNA binding protein that functions in pre-rRNA and pre-mRNA surveillance and in noncoding RNA degradation (Milligan et al., 2008). A second nuclear RNA exosome cofactor, Rrp47, is believed to act as a scaffolding protein that functions in RNA substrate recruitment and targeting to the exosome ribonuclease subunit, Rrp6 (Mitchell et al., 2003). Together, these nuclear RNA exosome cofactors recruit a third and critical nuclear RNA exosome cofactor, Mtr4, which is an RNA helicase, to the RNA exosome: Mpp6 tethers Mtr4 by contacting the Rrp40 exosome subunit and Rrp47 associates with the N-terminus of Rrp6 to form a surface that binds a helix of Mtr4 (Weick et al., 2018). The cytoplasmic RNA exosome cofactor, the Ski complex, is composed of four Ski proteins and assists the cytoplasmic exosome in the degradation of aberrant mRNAs in the cytoplasm (Mitchell, 2014).

The RNA exosome is highly conserved and was first identified and studied in the budding yeast, *S. cerevisiae* (Mitchell et al., 1997). As shown in Figure 1, the core RNA exosome complex is composed of ten subunits: six subunits form a barrel-like ring structure, three subunits form a cap structure at the top, and one catalytic subunit with both 3’ to 5’ exoribonuclease and endoribonuclease activity is located at the bottom. RNAs can be threaded through the central channel of the barrel to the exoribonuclease at the bottom to be degraded or processed (Zinder and Lima, 2017). The RNA exosome is highly conserved, and the subunits and structure of the human and yeast RNA exosome are similar (Wasmuth and Lima, 2012). The human RNA exosome subunits are termed exosome component (EXOSC) proteins and the *S. cerevisiae* RNA

exosome subunits are termed Rrp proteins after the original yeast genetic screen for ribosomal RNA processing (*rrp*) mutants in which they were identified (Mitchell et al., 1996, 1997).

Highlighting the critical function of the RNA exosome complex, several recent studies have identified mutations in the *EXOSC* genes encoding structural RNA exosome subunits that cause human disease (Morton et al., 2018). For example, mutations in the *EXOSC3* gene, which encodes a cap subunit of the RNA exosome, cause pontocerebellar hypoplasia type 1b (PCH1b), an autosomal-recessive, neurodegenerative disease (Wan et al., 2012). This finding was surprising as most of the RNA exosome subunit genes are essential in the organisms studied thus far (Allmang et al., 1999). In fact, the *EXOSC* mutations that are associated with disease are not predominantly null alleles but rather missense mutations that encode single amino acid changes. How these amino acid changes impact the function of the specific subunits or the overall function of the RNA exosome complex is not known.

Mutations in the *EXOSC2* gene, which encodes another cap subunit of the RNA exosome, have been linked to a novel syndrome characterized by retinitis pigmentosa, progressive hearing loss, premature aging, short stature, mild intellectual disability and distinctive gestalt (Di Donato et al., 2016), later named SHRF (Short stature, Hearing loss, Retinitis pigmentosa and distinctive Facies) syndrome (Yang et al., 2020). Using whole exome sequencing of three similarly affected patients (Figure 2), the study identified mutations in the *EXOSC2* gene that alter conserved amino acids (Di Donato et al., 2016). Interestingly, although the *EXOSC2* and *EXOSC3* genes both encode

RNA exosome cap subunits, mutations in these genes cause diseases in humans with distinct clinical presentation.

The amino acid substitutions in EXOSC2 that cause this novel syndrome have been identified, but how these amino acid changes impact RNA exosome function is unknown. The aim of this project was to analyze the functional consequences of the amino acid substitutions linked to this novel syndrome using the *S. cerevisiae* ortholog of EXOSC2, Rrp4, in budding yeast. Structural modelling (Figure 4) has provided some insight into how the amino acid substitutions affect protein folding, but they cannot predict how the changes affect cell function. We performed experiment using budding yeast as a model system to rapidly assess the consequences of mutations in the EXOSC2 subunit. After generation of the *rrp4* variants that model the *EXOSC2* variants identified in disease, we analyzed the growth of the *rrp4* mutant yeast cells, the levels of the rrp4 protein variants, the steady-state levels of several RNA exosome target transcripts in the *rrp4* mutant cells, and the genetic interactions of the *rrp4* mutants with known exosome cofactor mutants. We expressed these rrp4 variants, which model the pathogenic amino acid substitution in EXOSC2, as the sole copy of the essential Rrp4 protein in budding yeast. The results show that the yeast *rrp4-G58V* variant, corresponding to the *EXOSC2*-G30V, variant is lethal, whereas the yeast *rrp4-G226D* variant, corresponding to the *EXOSC2*-G198D variant, causes impaired cell growth, reduced Rrp4 protein levels, elevated levels of exosome RNA substrates, and demonstrates genetic interactions with exosome cofactor mutants. Taken together, these studies provide insight into how specific amino acid changes in EXOSC2 could impact RNA exosome function and contribute to disease pathology.

# MATERIALS AND METHODS

## *S. cerevisiae* strains, plasmids, and chemicals

All chemicals used in this study were obtained from Sigma-Aldrich (St. Louis, MO), United States Biological (Swampscott, MA), or Fisher Scientific (Pittsburgh, PA), unless otherwise noted. All media were prepared by standard procedures (Adams et al., 1997). Molecular cloning followed standard procedures (Sambrook et al., 1989). The *rrp4Δ* strain yAV1104 was previously described (Schaeffer et al., 2009).

## *S. cerevisiae* transformation

All yeast transformations were performed according to the standard Lithium Acetate (LiOAc) protocol (Burke et al., 2000). Cells were grown overnight to saturation in a 30˚C incubator in liquid YEPD (1% yeast extract, 2% peptone, 2% dextrose, in distilled water). Cell concentrations were normalized to $OD_{600}$ = 0.4 in 10 mL YEPD then incubated at 30˚C for 5 hours. The cells were washed with TE/LiOAc then resuspended in TE/LiOAc to a concentration of 2 x $10^9$ cells/mL. To these cells, plasmid DNA, single-stranded carrier DNA, and PEG/TE/LiOAc were added. The cells were agitated for 30 minutes at 30˚C before adding DMSO. The cells were heat shocked at 42˚C for 15 minutes, washed, and plated onto selective media

## *S. cerevisiae* cell growth assays

To test the *in vivo* function of *rrp4* mutants, *rrp4Δ* cells containing *RRP4-Myc* or *rrp4-Myc* mutant plasmid were serially diluted, spotted, and grown on solid medium plates, or the cells were grown in liquid medium as the optical density of the cultures

was measured over time using a microplate reader. For solid media assays, cells containing only Rrp4-Myc, rrp4-G58A-Myc, rrp4-G58V-Myc, or rrp4-G226D-Myc plasmid were grown overnight to saturation in a 30˚C incubator in Leu- minimal media. Cell concentrations were normalized to $OD_{600}$ = 1, serially diluted in 10-fold dilutions, then spotted onto Leu- minimal media plates and grown at 25˚, 30˚ and 37˚C. Plates were imaged daily for up to 5 days of growth. In the plasmid shuffle assay, *rrp4Δ* cells containing *RRP4-Myc, rrp4-Myc* mutant, or vector plasmid and *RRP4 URA3* maintenance plasmid were grown overnight to saturation in a 30˚C incubator in Ura-Leu- minimal medium. Cell concentrations were normalized to $OD_{600}$ = 1, serially diluted in 10-fold dilutions, then spotted onto Ura-Leu- minimal media plates or Leu- minimal media plates containing 5-fluoroorotic acid (5-FOA), and grown at 25˚, 30˚ and 37˚C. For liquid media assays, cells containing only Rrp4-Myc, rrp4-G58A-Myc, rrp4-G58V-Myc, or rrp4-G226D-Myc plasmid were grown overnight to saturation in a 30˚C incubator in Leu- minimal medium. Cells were diluted to an initial $OD_{600}$ = 0.01 in Leu- minimal media in a 96 well plate at 30˚C or 37˚C. The optical density of the liquid cultures was measured every 30 minutes and recorded in a BioTek SynergyMx microplate reader with Gen5 v2.04 software over 48 hours. Technical triplicates of each strain were measured, and the average of these triplicates was graphed. Error bars represent the standard error of the mean of three biological replicates.

**Immunoblotting**

To analyze the C-terminally Myc-tagged Rrp4 and mutant rrp4 protein expression levels, *rrp4Δ* cells expressing Rrp4-Myc, rrp4-G58A-Myc, rrp4-G58V-Myc, or rrp4-G226D-Myc protein were grown in 2 mL of Leu- minimal medium overnight at 30˚C to

saturation. Cells from these cultures were diluted in 10 mL of Leu- minimal media to an $OD_{600}$ = 0.4, then these cultures were grown for 5 hours at 37˚C. The cultures were centrifuged for 3 minutes at 3000 RPM to collect cells, then the pellets were transferred to 2 mL screw cap tubes.

Yeast cell lysates were prepared by resuspending centrifuged cell pellets in 0.3 mL of RPA-2 Buffer (50 mM Tris-HCl, pH 8; 150 mM NaCl; 0.5% sodium deoxycholate; 1% NP40; 0.1% SDS) supplemented with protease inhibitors [1 mM PMSF; 3 ng/ml PLAC (pepstatin A, leupeptin, aprotinin, and chymostatin)], and 300 µl of glass beads. Cells were disrupted in a Mini Bead Beater 16 Cell Disrupter (Biospec) for 4 × 1 min at 25° with 1 minute rest on ice between repetitions, and then centrifuged at 13,000 × g for 15 min at 4°. Protein lysate concentration was determined by Pierce BCA Protein Assay Kit (Life Technologies). Whole cell lysate protein samples (40 µg) were resolved on Criterion 4–20% gradient denaturing gels (Bio-Rad), transferred to nitrocellulose membranes (Bio-Rad) and Myc-tagged Rrp4 proteins were detected with anti-Myc monoclonal antibody 9B11 (1:2000; Cell Signaling). 3-phosphoglycerate kinase (Pgk1) protein was detected using anti-Pgk1 monoclonal antibody (1:30,000; Invitrogen) as a loading control.

**Total RNA isolation**

Cells containing *RRP4-Myc, rrp4-G58A-Myc,* or *rrp4-G226D-Myc* plasmids were grown in 2 mL of Leu- minimal medium overnight at 30˚C to saturation. Cells from these cultures were diluted in 10 mL of Leu- minimal media to an $OD_{600}$ = 0.4, then these cultures were grown for 5 hours at 30˚C. The cultures were centrifuged for 3 minutes at 3000 RPM to collect cells, then the pellets were transferred to 2 mL screw cap tubes.

Cell pellets were resuspended in 1 mL TRIzol (Invitrogen) with 300 µL of glass beads. Cell samples were disrupted in a Biospec Mini Bead Beater 16 Cell Disrupter for 2 minutes at 25˚C. 100 µL of 1-bromo-3-chloropropane (BCP) was added to each sample which was then vortexed for 15 seconds and incubated at 25˚C for 2 minutes. The samples were centrifuged at 16,300 x g for 8 minutes at 4˚C, and the upper layer was transferred to a fresh microfuge tube. 500 µL of isopropanol was used to precipitate the RNA, then the sample was vortexed for 10 seconds to mix. Total RNA was pelleted by centrifugation at 16,300 × g for 8 min at 4˚, then the RNA pellet was washed with 1 ml of 75% ethanol, centrifuged at 16,300 × g for 5 min at 4˚, and air-dried for 15 min. Total RNA was resuspended in 50 µl diethylpyrocarbonate (DEPC, Sigma)-treated water, and stored at −80°.

**Quantitative RT-PCR**

To analyze *snR44, snR128, U4* snRNA*, U6* snRNA*, TLC1* ncRNA*, NEL025c* CUT*,* CUT *638,* and CUT *273* steady state RNA levels, *rrp4*Δ cells containing *RRP4-Myc, rrp4-G58A-Myc*, or *rrp4-G226D-Myc* plasmids were grown in 2 mL of Leu- minimal medium overnight at 30˚C to saturation. Cells from these cultures were diluted in 10 mL of Leu- minimal media to an $OD_{600}$ = 0.4, then these cultures were grown for 5 hours at 30˚C. The cultures were centrifuged for 3 minutes at 3000 RPM to collect cells, then the pellets were transferred to 2 mL screw cap tubes. After total RNA isolation, 1 µg of RNA was reverse transcribed to make cDNA using the M-MLV Reverse Transcriptase (Invitrogen) according to the manufacturer's protocol. Quantitative PCR was performed on technical triplicates of 10 ng cDNA from three biologically independent samples using 0.5 µM *snR44, snR128, U4* snRNA*, U6* snRNA*. TLC1* ncRNA*, NEL025c* CUT*,*

CUT *638,* CUT *273* primers, and control *ALG9* primers, and QuantiTect SYBR Green PCR master mix (Qiagen) on a StepOnePlus Real-Time PCR machine (Applied Biosystems; $T_{anneal}$: 55˚C; 44 cycles). The mean RNA levels were calculated by the ΔΔCt method (Livak and Schmittigen, 2001) then normalized to the mean RNA levels in *RRP4* cells. These values were converted to fold changes relative to *RRP4* levels, and error bars represent the standard error of the mean.

## RESULTS

### Novel syndrome patient mutations alter conserved EXOSC2 residues

To assess the functional consequences of the SHRF-associated EXOSC2-G30V and EXOSC2-G198D substitutions, we generated the corresponding amino acid changes in the *S. cerevisiae* ortholog, Rrp4*.* These amino acid substitutions occur in highly conserved residues of EXOSC2/Rrp4. Figure 2 shows the human EXOSC2 and *S. cerevisiae* Rrp4 protein domain structures and highlights the conserved residues altered in disease and the sequences flanking these residues among the EXOSC2/Rrp4 orthologs. Importantly, the *S. cerevisiae* RNA exosome has been extensively characterized in budding yeast and shown to be both structurally and functionally similar to the human RNA exosome (Sloan et al., 2012). We created the following rrp4 variants: rrp4-G58V - corresponding to EXOSC2-G30V identified in disease, rrp4-G58A - an alternative rrp4 variant that models a different amino acid change at the conserved EXOSC2 G30 position that was not identified in disease, and rrp4-G226D - corresponding to EXOSC2-G198D identified in disease. These rrp4 variants were used

to assess the functional consequences of disease-linked amino acid substitutions in the Rrp4 exosome subunit.

**Amino acid substitutions in *S. cerevisiae* Rrp4 corresponding to SHRF-associated EXOSC2 substitutions impair growth**

To test whether the *rrp4* variants corresponding to the *EXOSC2* variants identified in disease could complement the growth of a *rrp4*Δ yeast strain, which would normally die as *RRP4* is an essential gene (Mitchell et al., 1996), we transformed *rrp4* variant plasmids into *rrp4*Δ cells and assessed their growth in solid and liquid media assays. The *rrp4*Δ cells containing an *RRP4 URA3* maintenance plasmid, which maintains viability, were transformed with empty vector (pAC3), *RRP4, rrp4-G58V* or *rrp4-G198D LEU2* test plasmid. In a plasmid shuffle assay, *rrp4*Δ cells containing the *RRP4 URA3* maintenance plasmid and *R/rrp4 LEU2* test plasmid were serially diluted and spotted onto solid media plates that contains 5-fluoroorotic acid (5-FOA), which selects against cells that harbor the *RRP4 URA3* maintenance plasmid, and lack leucine, which selects for cells that contain the *RRP4/rrp4 LEU2* test plasmid. As a control for equal serial dilution/cell numbers, the cells were also spotted onto Ura- Leu- media plates that select for cells containing both maintenance and test plasmid. The solid media plates were incubated at 25˚C, 30˚C and 37˚C. On 5-FOA, the *rrp4-G30V* mutant cells are not viable at any temperature, whereas the *rrp4-G226D* cells exhibit a growth defect compared to wildtype *RRP4* cells at 30˚C and 37˚C (Figure 5A).

As the *rrp4-G58V* variant was found to be lethal, we generated an alternative *rrp4* variant, *rrp4-G58A,* to test the effect of a different amino acid change at the

conserved Rrp4 G58 position corresponding to the EXOSC2 G30 position. Alanine was selected as the next smallest nonpolar amino acid after valine to replace the glycine residue in the N-terminal domain of Rrp4. Surprisingly, on 5-FOA, while the *rrp4-G58V* mutant cells are not viable at any temperature, *rrp4-G58A* mutant cells grow similarly to wildtype *RRP4* cells at all temperatures in the solid media plasmid shuffle assay (Figure 5B).

The impaired growth of *rrp4-G226D* mutant cells at 30˚C and 37˚C was verified quantitatively in a liquid media growth assay (Figures 6A and 6B). Consistent with the solid media assay results, the *rrp4-G226D* cells grow more slowly compared wildtype *RRP4* cells at 30˚C (Figure 6A) and exhibit an even more pronounced growth defect at 37˚C (Figure 6B). As with the solid media growth assay, growth of the *rrp4-G58A* mutant cells is indistinguishable from wildtype *RRP4* cell growth at all temperatures.

**Rrp4 protein variants are expressed at similar levels to wildtype Rrp4**

To determine whether the growth defects of the *rrp4* mutant cells are due to changes in the level of the rrp4 protein variants relative to wildtype Rrp4 protein, we examined the steady-state expression of Myc-tagged wildtype Rrp4 and rrp4-G226D as sole copy of the Rrp4 protein in *rrp4*Δ cells grown at 30˚C and 37˚C using immunoblotting. The level of rrp4-G226D protein variant is similar to the level of wildtype Rrp4 at both temperatures (Figure 7A).

To determine the expression level of rrp4-G58V protein variant, which cannot support growth of *rrp4*Δ cells alone, we examined the expression of Myc-tagged Rrp4, rrp4-G58V, and other rrp4 variants in *rrp4*Δ cells containing the *RRP4 URA3*

maintenance plasmid grown 30˚C and 37˚C. The expression level of the rrp4-G58V variant is 68% compared to that of wildtype Rrp4 (Figure 7B). The expression level of the rrp4-G226D variant is 51% compared to that of wildtype Rrp4 (Figure 7B).

**RNA Exosome target transcripts are elevated in *rrp4-G226D* mutant cells**

To determine whether the *rrp4* variants cause changes in RNA exosome function, we measured the steady-state levels of several known RNA exosome substrates (Wasmuth and Lima, 2012) in *rrp4* mutant cells using quantitative RT-PCR. Specifically, we examined the levels of snRNAs (*U4*, *U6*), snoRNAs (*snR44*, *snR128*), ncRNAs (*TLC1* telomerase RNA, *SCR1* signal recognition particle RNA), and Cryptic Unstable Transcripts (CUTs: *NEL025c*, *CUT273*, *CUT638*) in *RRP4*, *rrp4-G58A*, and *rrp4-G226D* cells grown at 37°CThe *rrp4-G226D* mutant cells exhibit a statistically significant increase in levels of *U4* snRNA, *TLC1* telomerase RNA, and *CUT273* ncRNA (Figure 8).

**The *rrp4-G226D* mutant shows genetic interactions with RNA exosome cofactors**

The specificity of the RNA exosome for distinct RNA substrates is thought to be conferred by several exosome cofactors, which facilitate processing and degradation (Fasken et al., 2020). To determine whether the *rrp4-G226D* variant exhibits genetic interactions with exosome cofactor mutants, we deleted the non-essential, nuclear exosome cofactor genes *MPP6* and *RRP47* in the *rrp4*Δ strain via homologous recombination, yielding *rrp4*Δ *mpp6*Δ and *rrp4*Δ *rrp47*Δ double mutant strains. In addition, using an *MTR4 RRP4 URA3* maintenance plasmid, we deleted the essential, nuclear exosome cofactor gene *MTR4* and the *RRP4* gene in a wildtype strain, yielding an *rrp4*Δ

*mtr4*Δ double mutant strain. We examined the growth of *rrp4-G226D mpp6*Δ, *rrp4-G226D rrp47*Δ, and *rrp4-G226D mtr4* double mutant cells relative to *rrp4-G226D* cells alone in a solid media growth assay.

The *rrp4-G226D mpp6*Δ cells exhibit slower growth compared to *rrp4-G226D* cells at all temperatures tested, indicating that deletion of *MPP6* exacerbates the growth defect of *rrp4-G226D* cells (Figure 9A). The *rrp4-G226D rrp47*Δ cells also show slower growth relative to *rrp4-G226D* cells at all temperatures tested, indicating that deletion of *RRP47* also enhances the growth defect of *rrp4-G226D* cells (Figure 9A). Notably, the *rrp4-G226D rrp47*Δ cells grow more slowly than the *rrp4-G226D mpp6*Δ cells; however this difference is predominantly due to the fact the *rrp47*Δ mutant cells exhibit a growth defect, but *mpp6*Δ cells do not (Figure 9A). The *rrp4-G226D mtr4*Δ cells expressing different *mtr4* missense variants do not exhibit growth that is different relative to *rrp4-G226D* cells (Figure 9B). These data indicate that the *rrp4-G226D* variant shows negative genetic interactions with *MPP6* and *RRP47* exosome cofactor mutants but does not exhibit genetic interactions with *MTR4* exosome cofactor mutants.

**Expression of Heat shock protein 82 does not rescue *rrp4-G226D* growth defect**

To investigate whether the temperature-sensitive growth of *rrp4-G226D* cells could be rescued by expression of a chaperone protein, *rrp4Δ* cells containing wildtype *RRP4* or *rrp4-G226D* test plasmid were transformed with empty vector (pAC4) or plasmid containing the heat shock protein 82 (*HSP82*) gene. Cells were serially diluted and spotted onto Leu- plates. The growth of *rrp4-G226D* cells expressing *HSP82* was not improved at 37°C compared to *rrp4-G226D* cells containing empty vector (Figure

10). In fact, the growth of *rrp4-G226D* cells expressing *HSP82* was further impaired at 37°C relative to *rrp4-G226D* cells containing empty vector (Figure 10).

## DISCUSSION

This study characterized the functional consequences of amino acid substitutions in the budding yeast ortholog of EXOSC2, Rrp4. When expressed as the sole copy of the essential Rrp4 protein, the rrp4-G58V variant is not functional while the rrp4-G226D variant impairs cellular growth and function. This result was surprising given the genotypes and phenotypes of SHRF patients (Figure 2A). All patients in the study identifying *EXOSC2* mutations as causing the novel syndrome share the G30V missense variant: two patients were homozygous for the G30V variant and the third patient was heterozygous with one allele of EXOSC2 encoding the G198D variant and the other allele encoding the G30V variant (Di Donato et al., 2016). Given that the G30V mutation had a greater frequency in the patients studied and in the control group tested, it was hypothesized that it may be less debilitating to RNA exosome function than the rarer G198D mutation, but the results of this study suggest otherwise at least for the budding yeast model.

A puzzling result from this project was the stark difference in phenotypes of *rrp4-G58A* and *rrp4-G58V* mutant cells (Figure 5B). As mentioned above, the rrp4-G58V models a patient allele. We created the rrp4-G58A to explore why such a subtle change might completely eliminate the function of the Rrp4 protein. Cells expressing the *rrp4-G58V* variant were not viable at any temperature, whereas *rrp4-G58A* cells grew similarly to wildtype *RRP4* cells. The change from glycine to valine at position 30 is

thought to shorten the interatomic distance between this EXOSC2 residue and neighboring amino acids of EXOSC4 which includes Asp154 (Di Donato et al., 2016). Substituting Gly30 with an amino acid slightly smaller than valine, alanine, may reduce the unfavorable interactions between the nonpolar EXOSC2 residue and the negatively charged EXOSC4 residue. Additionally, glycine is the only amino acid with a non-chiral R group. Replacing glycine with a less conformationally flexible amino acid such as valine may prevent formation of a kink in the backbone peptide chain which could be necessary for normal function.

The results from these experiments can be used to begin building a model to explain the mechanism underlying patient phenotypes. Disease-linked amino acid substitutions in the EXOSC2 subunit could alter RNA exosome function by three potential mechanisms: a) differentially affect interactions with co-factors or the ribonuclease subunit itself; b) differentially affects the level and stability of the subunit, resulting in changes in the assembly and disassembly of the complex; and/or c) affects the entry paths and interactions with specific RNA (Figure 11). The observed functional consequences likely result from a combination of the three listed mechanisms, and further studies can help to define the functional consequences of pathogenic amino acid substitutions.

The first mechanism proposes that RNA exosome cofactors confer specificity for certain target RNA transcripts, so the amino acid substitutions in different RNA exosome subunits could then selectively disrupt cofactor interaction(s). This mechanism could explain the distinct, tissue specific disease phenotypes seen in patients. My data show that deleting exosome cofactor genes  further impairs growth of the temperature-

sensitive *rrp4-G226D* mutant, but to different extents based on the cofactor deleted (Figure 9A). qRT-PCR could be used to test whether this reduced growth is caused by a greater increase in steady-state RNA levels compared to mutant cells that contain the cofactors. Such an experiment could also provide insight into which RNA targets are critical to confer the functional defects.

Another possibility is that amino acid substitutions could affect the overall Rrp4 protein level which could explain the reduced growth of mutant cells. To test this hypothesis, I used immunoblotting. The resulting blot reveals that rrp4-G226D mutant protein is expressed, but at a reduced level compared to wildtype Rrp4 (Figure 7). This result could indicate that the cell has a way to differentially express the wildtype protein over the mutant or that the mutant protein is unstable or more rapidly degraded than the wildtype protein. Mis-assembly of the RNA exosome complex could be tested using a native gel. As the protein complexes are not denatured in a native gel, the natural structure of the analyte would be fully retained. The wildtype version could then be compared to the mutants to test whether the RNA exosome is altered in *rrp4-G226D* cells. Biochemical techniques such as immunoprecipitation could also be used to compare association of the wildtype and mutant RRP4 proteins with the overall RNA exosome complex.

Finally, the third mechanism explores potentially disrupted interactions and entry of RNA substrates when the RNA exosome has a mutated subunit. The *rrp4-G226D* mutants show altered steady state levels of several target mRNA substrates, but not all transcripts tested (Figure 8). This finding could indicate that the G226D mutation impairs the exosome-mediated RNA processing in a specific manner rather than generally

reducing exosome activity. To extend my qRT-PCR analysis of RNA exosome mediated RNA processing, our lab is analyzing RNA-Seq data to identify broader trends in RNA processing defects.

We attempted one approach to explore potential therapeutic approaches to restore Rrp4/EXOSC2 function. As shown in Figure 10, the chaperone protein HSP82 failed to rescue the temperature sensitive growth defect exhibited by cells expressing rrp4-G226D variant protein. Hsp82 is a heat shock protein that is expressed when cells are exposed to elevated temperatures or other stressors, allowing cells to better tolerate extreme temperature conditions (Borkovich et al., 1989). Based on some recent work suggesting that such chaperones might be able to suppress growth defects (Karras et al., 2017), I tested the hypothesis that overexpressing HSP82 could rescue the growth defect in *rrp4-G226D* cells, but overexpression did not improve cell growth (Figure 10).

The methodology used in this thesis to characterize amino acid substitutions in EXOSC2 can be applied to the study of other RNA exosome subunits. In addition to the aforementioned amino acid substitutions linked to disease in EXOSC2 and EXOSC3, mutations have been found in EXOSC5, EXOSC8, and EXOSC9 that result in distinct diseases. I have contributed to a publication characterizing missense mutations in EXOSC5 that is currently being reviewed. We have also been working on a comparative study to begin to understand how these different amino acid substitutions in different RNA exosome subunits differentially impact RNA exosome function (data not shown). The results of this work will provide insight on RNA exosome function with the eventual aim of improving patient outcomes. By employing a yeast system, we can rapidly and cost-effectively assess how amino acid changes alter RNA exosome function in a

controlled, well characterized genetic background. We can also use the power of yeast genetics to investigate interactions of the RNA exosome with other proteins. My work provides a basis for future study in higher order model organisms to develop improved patient therapeutics.

## REFERENCES


1. Adams, A., Gottschling, D.E., Kaiser, C.A., and Steams, T. (1997). Methods in Yeast Genetics (Cold Spring Harbor, NY: Cold Spring Harbor Laboratory Press).

2. Allmang, C., Petfalski, E., Podtelejnikov, A., Mann, M., Tollervey, D., and Mitchell, P. (1999). The yeast exosome and human PM–Scl are related complexes of 3′ → 5′ exonucleases. Genes Dev. *13*, 2148.

3. Borkovich, K.A., Farrelly, F.W., Finkelstein, D.B., Taulien, J., and Lindquist, S. (1989). hsp82 is an essential protein that is required in higher concentrations for growth of cells at higher temperatures. Mol. Cell. Biol. *9*, 3919.

4. Burke, D., Dawson, D., and Steams, T. (2000). Methods in yeast genetics: a Cold Spring Harbor Laboratory course manual.

5. Di Donato, N., Neuhann, T., Kahlert, A.-K., Klink, B., Hackmann, K., Neuhann, I., Novotna, B., Schallner, J., Krause, C., Glass, I.A., et al. (2016). Mutations in EXOSC2 are associated with a novel syndrome characterised by retinitis pigmentosa, progressive hearing loss, premature ageing, short stature, mild intellectual disability and distinctive gestalt. J. Med. Genet. *53*, 419–425.

6. Fasken, M.B., Losh, J.S., Leung, S.W., Brutus, S., Avin, B., Vaught, J.C., Potter-Birriel, J., Craig, T., Conn, G.L., Mills-Lujan, K., et al. (2017). Insight into the RNA Exosome Complex Through Modeling Pontocerebellar Hypoplasia Type 1b Disease Mutations in Yeast. Genetics *205*, 221–237.

7. Fasken, M.B., Morton, D.J., Kuiper, E.G., Jones, S.K., Leung, S.W., and Corbett, A.H. (2020). The RNA Exosome and Human Disease. Eukaryot. RNA Exosome 3–33.

8. Karras, G.I., Yi, S., Sahni, N., Fischer, M., Xie, J., Vidal, M., Alan D'Andrea, Whitesell, L., and Lindquist, S. (2017). HSP90 Shapes the Consequences of Human Genetic Variation. Cell *168*, 856-866.e12.

9. Kilchert, C., Wittmann, S., and Vasiljeva, L. (2016). The regulation and functions of the nuclear RNA exosome complex. Nat. Rev. Mol. Cell Biol. *17*, 227–239.

10. Livak, K.J., and Schmittigen, T.D. (2001). Analysis of relative gene expression data using real-time quantitative PCR and the 2(-Delta C(T)) Method. Methods *25*, 402–408.

11. Milligan, L., Decourty, L., Saveanu, C., Rappsilber, J., Ceulemans, H., Jacquier, A., and Tollervey, D. (2008). A Yeast Exosome Cofactor, Mpp6, Functions in RNA Surveillance and in the Degradation of Noncoding RNA Transcripts. Mol. Cell. Biol. *28*, 5446–5457.

12. Mitchell, P. (2014). Exosome Substrate Targeting: The Long and Short of It (Biochem Soc Trans).

13. Mitchell, P., Petfalski, E., and Tollervey, D. (1996). The 3' end of yeast 5.8S rRNA is generated by an exonuclease processing mechanism. Genes Dev. *10*, 502–513.

14. Mitchell, P., Petfalski, E., Shevchenko, A., Mann, M., and Tollervey, D. (1997). The Exosome: A Conserved Eukaryotic RNA Processing Complex Containing Multiple 3′→5′ Exoribonucleases. Cell *91*, 457–466.

15. Mitchell, P., Petfalski, E., Houalla, R., Podtelejnikov, A., Mann, M., and Tollervey, D. (2003). Rrp47p Is an Exosome-Associated Protein Required for the 3′ Processing of Stable RNAs. Mol. Cell. Biol. *23*, 6982–6992.

16. Morton, D.J., Kuiper, E.G., Jones, S.K., Leung, S.W., Corbett, A.H., and Fasken, M.B. (2018). The RNA exosome and RNA exosome-linked disease. RNA *24*, 127–142.

17. Sambrook, J., Fritsch, E.F., and Maniatis, T. (1989). Molecular Cloning: A Laboratory Manual (Cold Spring Harbor, NY: Cold Spring Harbor Laboratory Press).

18. Schaeffer, D., Tsanova, B., Barbas, A., Reis, F.P., Dastidar, E.G., Sanchez-Rotunno, M., Arraiano, C.M., and Hoof, A. van (2009). The exosome contains domains with specific endoribonuclease, exoribonuclease and cytoplasmic mRNA decay activities. Nat. Struct. Mol. Biol. *16*, 56.

19. Schaeffer, D., Clark, A., Klauer, A.A., Tsanova, B., and Hoof, A. van (2010). Functions of the Cytoplasmic Exosome. RNA Exosome 79–90.

20. Sloan, K.E., Schneider, C., and Watkins, N.J. (2012). Comparison of the yeast and human nuclear exosome complexes. Biochem. Soc. Trans. *40*, 850–855.

21. Wan, J., Yourshaw, M., Mamsa, H., Rudnik-Schöneborn, S., Menezes, M.P., Hong, J.E., Leong, D.W., Senderek, J., Salman, M.S., Chitayat, D., et al. (2012). Mutations in the RNA exosome component gene EXOSC3 cause pontocerebellar hypoplasia and spinal motor neuron degeneration. Nat. Genet. *44*, 704.

22. Wasmuth, E.V., and Lima, C.D. (2012). Chapter Three - Structure and Activities of the Eukaryotic RNA Exosome. In The Enzymes, G.F. Chanfreau, and F. Tamanoi, eds. (Academic Press), pp. 53–75.

23. Weick, E.-M., Puno, M.R., Januszyk, K., Zinder, J.C., DiMattia, M.A., and Lima, C.D. (2018). Helicase-dependent RNA decay illuminated by a cryo-EM structure of a human nuclear RNA exosome-MTR4 complex. Cell *173*, 1663.

24. Yang, X., Bayat, V., DiDonato, N., Zhao, Y., Zarnegar, B., Siprashvili, Z., Lopez-Pajares, V., Sun, T., Tao, S., Li, C., et al. (2020). Genetic and genomic studies of pathogenic EXOSC2 mutations in the newly described disease SHRF implicate the autophagy pathway in disease pathogenesis. Hum. Mol. Genet. *29*, 541–553.

25. Zinder, J.C., and Lima, C.D. (2017). Targeting RNA for processing or destruction by the eukaryotic RNA exosome and its cofactors. Genes Dev. *31*, 88–100.

## FIGURES

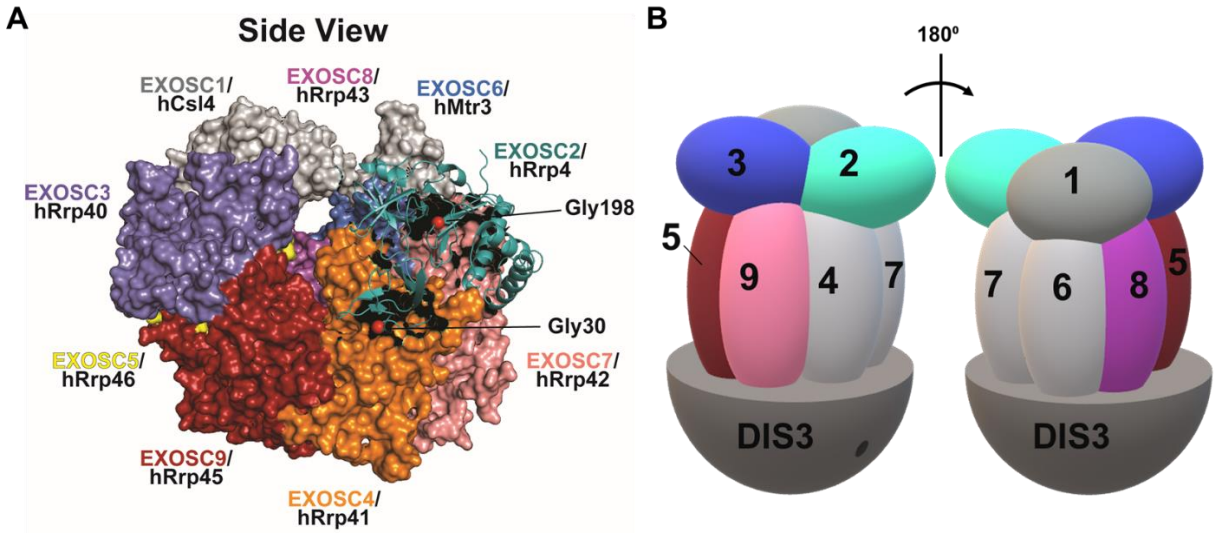


**Figure 1. RNA exosome structure.** (A) Crystal structure of the human RNA Exosome. The RNA Exosome is an essential, evolutionarily conserved complex composed of ten different subunits, nine of which are structural. There are three cap subunits: EXOSC1/Csl4 (Human/S. cerevisiae); EXOSC2/Rrp4; EXOSC3/Rrp40, six core subunits: EXOSC4/Rrp41; EXOSC5/Rrp46; EXOSC6/Mtr3; EXOSC7/Rrp42; EXOSC8/Rrp43; EXOSC9/Rrp45, and a catalytic base subunit: DIS3/Rrp44 (not pictured) (B) Cartoon schematic of RNA Exosome.

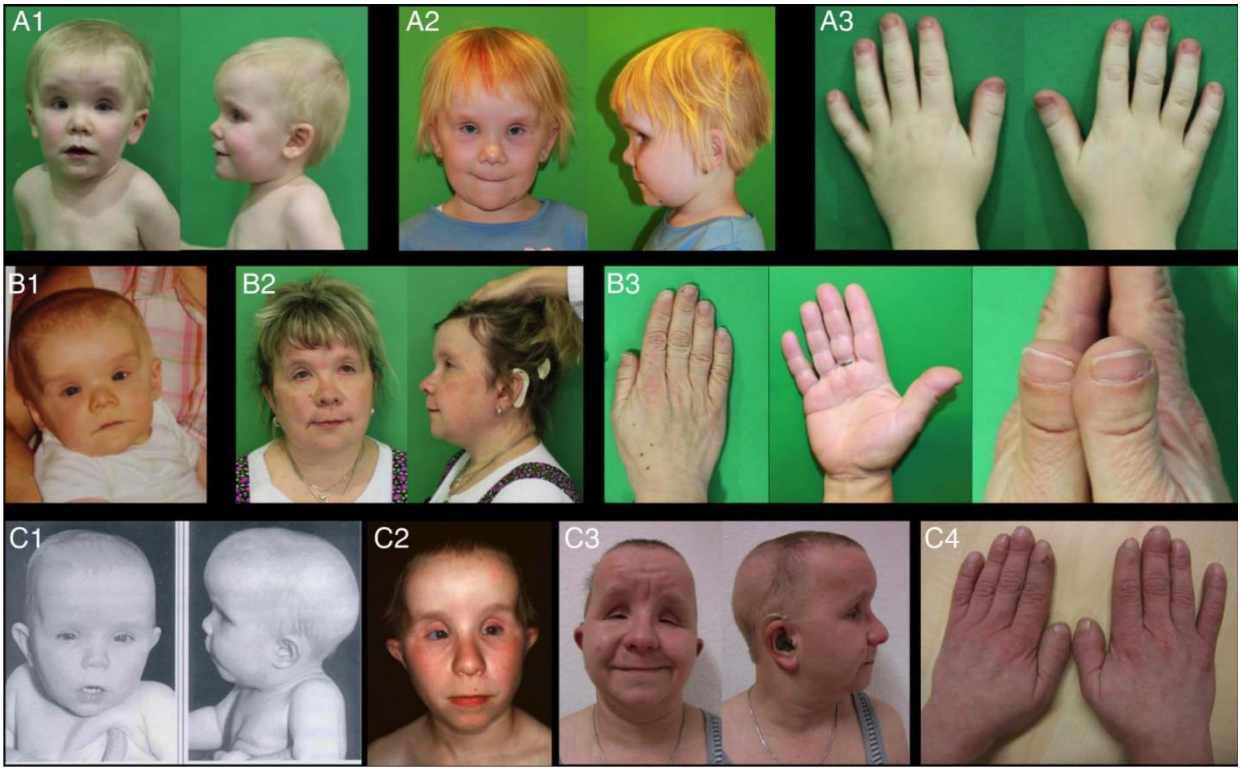


**Figure 2. Clinical pictures of patient phenotypes (Di Donato et al., 2016).** (A) Patient 1 at age 3 years (A1, A3) and age 6 years and 4 months (A2). (B) Patient 2 at age 1 year (B1) and 41 years (B2, B3). (C) Patient 3 at age 1 year (C1), 13 years (C2) and 28 years (C3, C4). Symptoms include high, prominent forehead, deep set eyes, short palpebral fissures, wide nasal base with broad nasal tip, long philtrum, sparse hair or partial alopecia in some patients, and brachydactyly with broad terminal phalanges.

**A**

| Exosome Subunit | Amino Acid Substitution | Patient Genotype | | Patient Phenotype | Disease Severity | Patient Number | Patient Lifespan |
|---|---|---|---|---|---|---|---|
| EXOSC2 | G30V | G30V | Homozygous | Novel Syndrome* | Mild | 2 | >44 yr |
| EXOSC2 | G198D | G198D/G30V | Heterozygous | Novel Syndrome* | Mild | 1 | >28 yr |

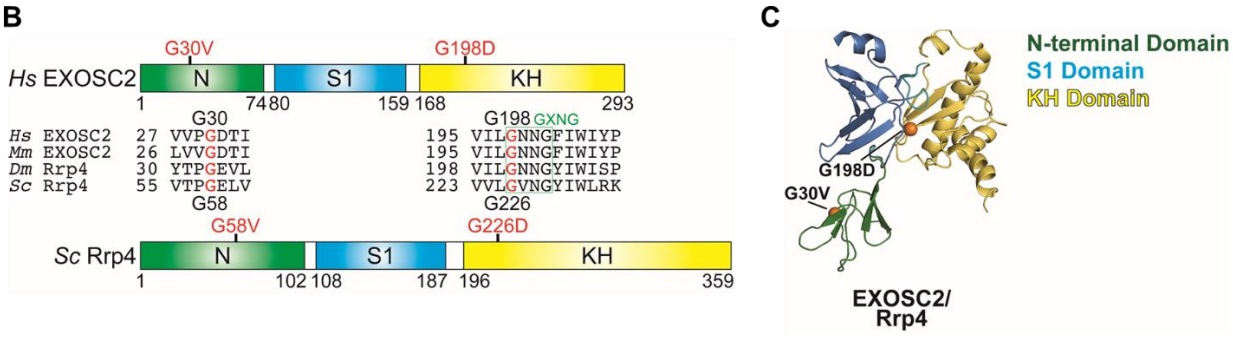


**Figure 3. Mutations in *EXOSC2* gene cause novel syndrome with retinitis pigmentosa.** (A) Mutations in exosome cap subunit gene, *EXOSC2*, identified in patients with novel syndrome that includes retinitis pigmentosa, hearing loss, premature aging, and mild intellectual disability. Whole exome sequencing of three patients identified mutations in the *EXOSC2* gene (Di Donato et al. J. Med. Genet. (2016)). (B) Domain of EXOSC2/Rrp4 highlights location of evolutionary conserved residues altered in disease. Domain structures of human EXOSC2 and *S. cerevisiae* ortholog, Rrp4, highlight location of conserved EXOSC2-G30 and -G198 residues altered in disease (G30V and G198D) and corresponding Rrp4-G58 and -G226 residues altered for functional analysis (G58V, G58A, G226D) in N-terminal domain and RNA binding KH domain, respectively. (C) Crystal structure of EXOSC2 alone with highlighted location of residues altered in disease (PDB:2NN6, Liu *et al*. Cell (2006)).

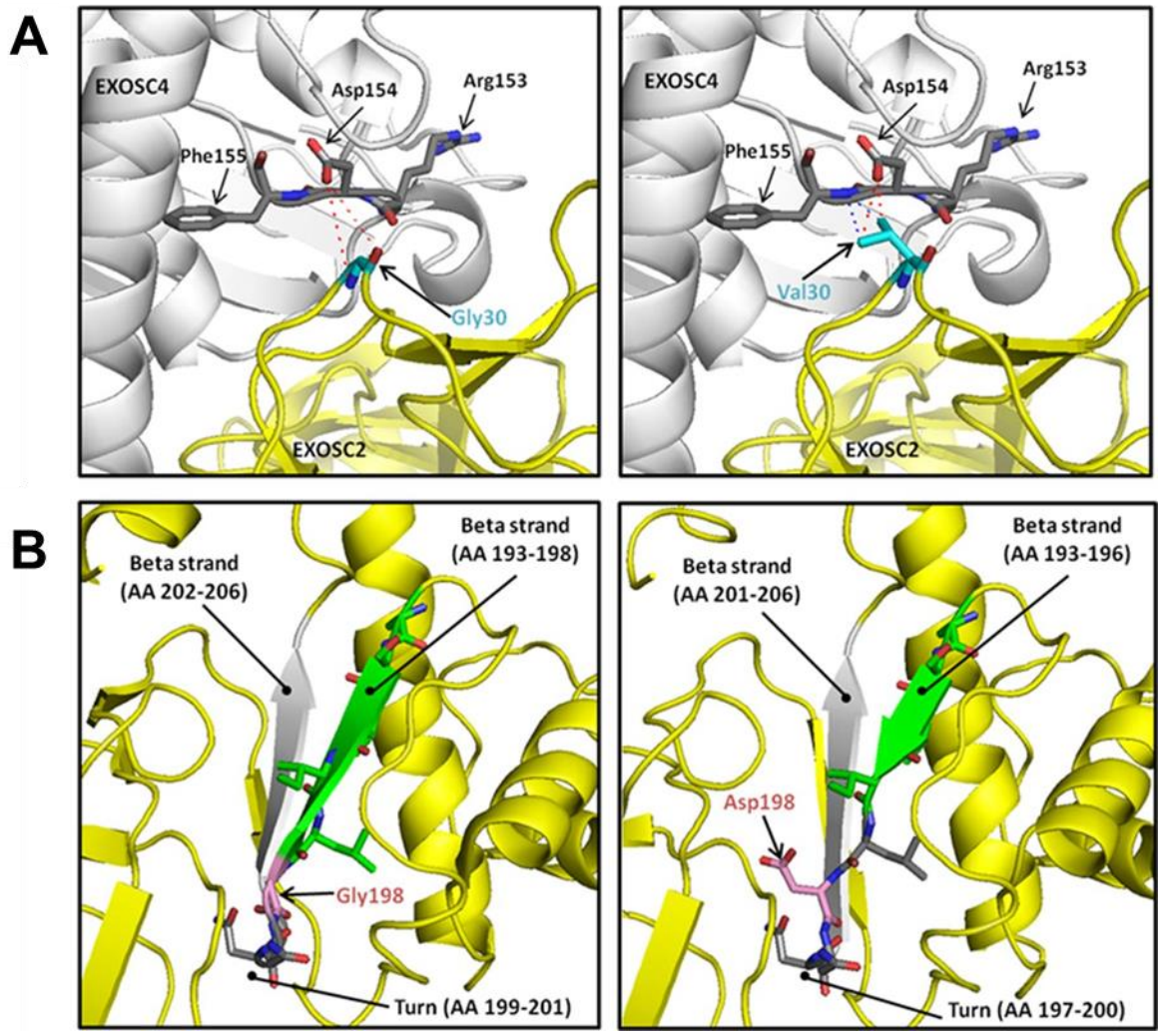


**Figure 4. Structural Modelling of EXOSC2 Amino Acid Substitutions. (Di Donato et al, 2016).** Models were generated using PyMOL molecular graphics software. (A) The first patient amino acid substitution replaces a glycine in the native structure (left) with valine in the mutant structure (right) which shortens the interatomic distance between the EXOSC2 and EXOSC4 subunits. (B) The second patient amino acid substitution replaces a glycine in the native structure (left) with aspartic acid in the mutant structure (right). This induces a conformational change that shortens a beta strand from six to four amino acids.

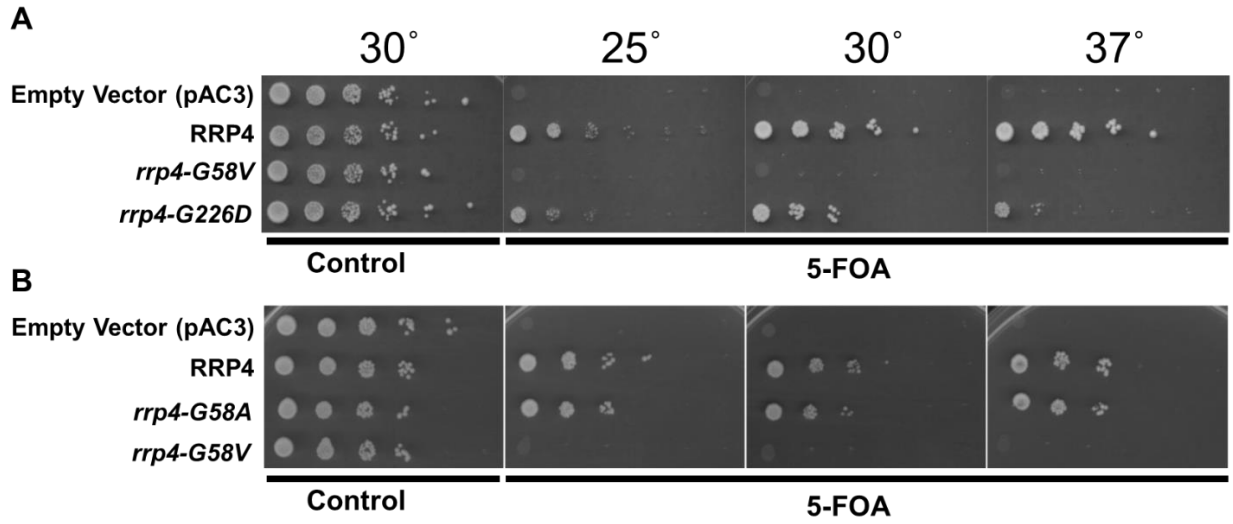


**Figure 5. The *rrp4-G58V* mutant yeast cells are not viable, whereas the *rrp4-G226D* mutant yeast cells exhibit impaired growth in a solid media growth assay.** (A) The *rrp4* mutant cells modelling patient amino acid substitutions show impaired growth on solid media. The *rrp4-G226D* mutant cells exhibit a growth defect at 37˚C, whereas the *rrp4-G58V* mutant is not functional at any temperature tested. The *rrp4*Δ cells containing *RRP4* maintenance plasmid and vector, wildtype *RRP4-Myc*, or *rrp4-Myc* mutant test plasmid were grown on control Ura- Leu- media to retain both maintenance and test plasmid or media containing 5-Fluoroorotic acid (5-FOA) that selects for cells that do not have the *URA3* maintenance plasmid and retain only test plasmid. (B) *rrp4-G58V* mutation is not functional whereas *rrp4-G58A* mutaant cells exhibit wildtype growth. *rrp4-G58A* mutant is not a patient mutation but was generated to study the lethal *rrp4-G58V* mutant. The *rrp4*Δ cells containing RRP4 maintenance plasmid and vector, wildtype RRP4-Myc, or rrp4-Myc mutant test plasmid were grown on control Ura- Leu- media that retains both maintenance and test plasmid or media containing 5-FOA that selects for cells that do not have the *URA3* maintenance plasmid and retain only test plasmid.

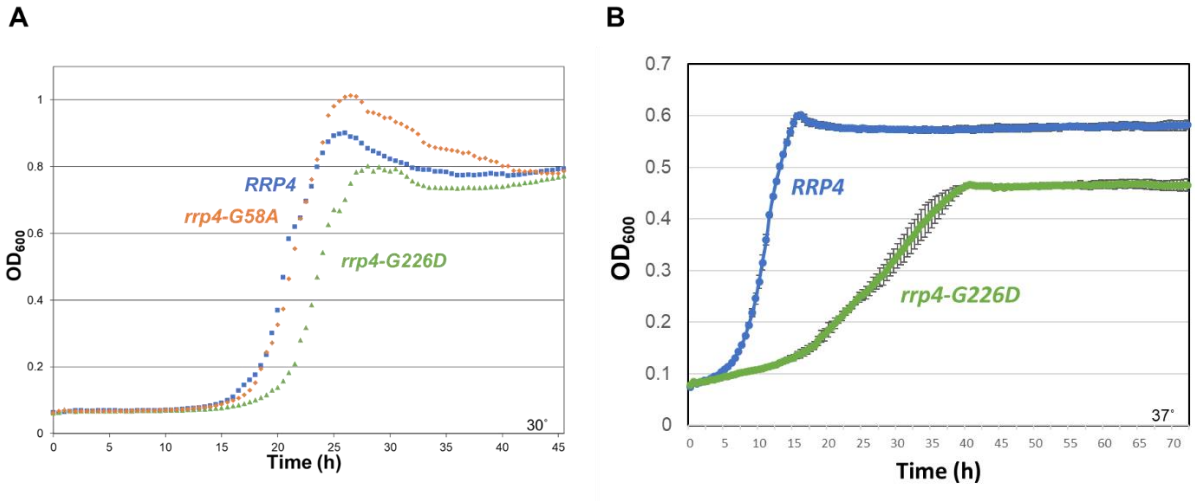


**Figure 6. The *rrp4-G226D* mutant yeast cells exhibit impaired growth in a liquid media growth assay.** (A) The *rrp4-G226D* mutant cells exhibit a growth defect compared to wildtype *RRP4* cells at 30˚C. In contrast, the *rrp4-G58A* mutant cells grow similarly to wildtype *RRP4* cells. (B) The *rrp4-G226D* mutant cells exhibit a growth defect at 37˚C compared to wildtype RRP4 cells. Curves represent the average of biological triplicates and error bars indicate standard error of the mean. The *rrp4*Δ cells containing only wildtype *RRP4-Myc* or *rrp4-Myc* mutant plasmid were grown in Leu- liquid media and optical density of cells was measured at OD600 every 30 min and graphically represented.

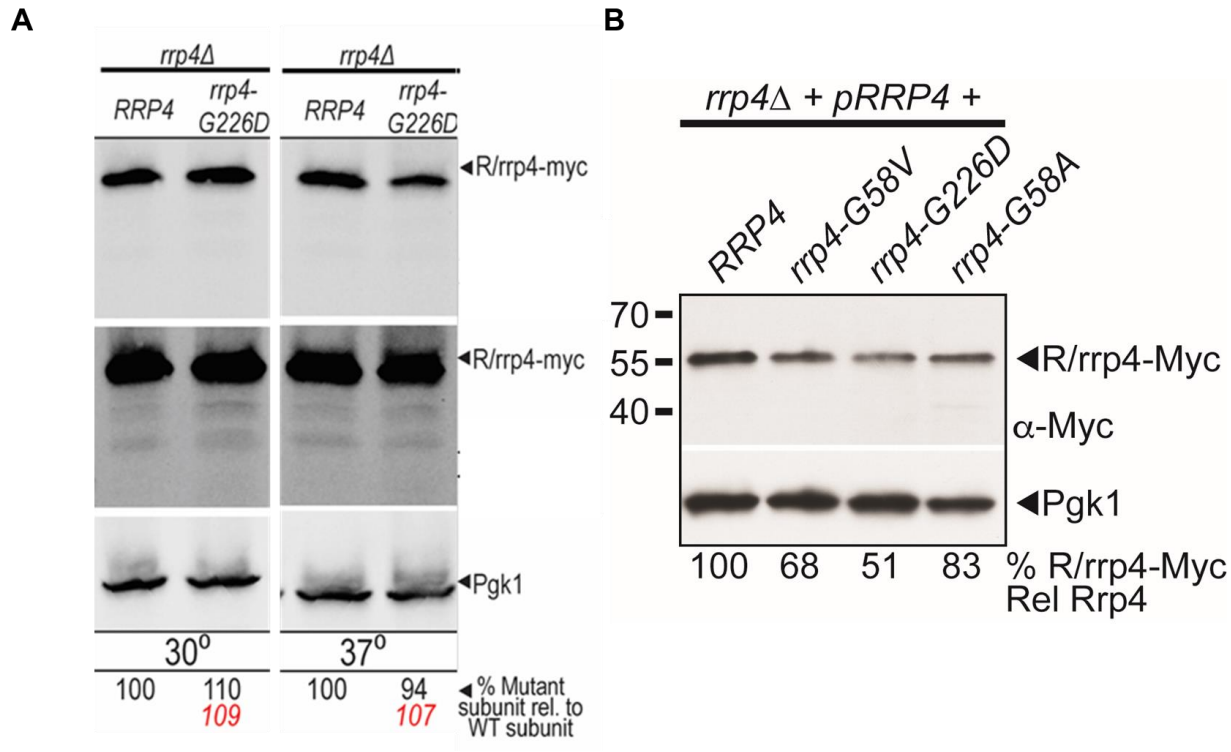


**Figure 7. The rrp4-G58V and rrp4-G226D protein variants are expressed.** (A) The Myc-tagged rrp4-G226D and rrp4-G58A-Myc mutant proteins are expressed in rrp4Δ cells alone. Myc-tagged R/rrp4-Myc proteins were detected by immunoblotting with anti-Myc antibody. The Pgk1 (3-Phosphoglycerate kinase) protein was detected as a loading control. Protein levels were quantitated and reported as % mutant subunit relative to wildtype subunit levels. Red text indicates subunit level normalized to PGK1 levels. (B) The Myc-tagged rrp4-G58V, rrp4-G226D, and rrp4-G58A mutant proteins are expressed in rrp4Δ cells containing RRP4 maintenance plasmid, but at reduced level compared to cells expressing wildtype Rrp4-Myc. Myc-tagged R/rrp4-Myc proteins were detected by immunoblotting with anti-Myc antibody. The Pgk1 (3-Phosphoglycerate kinase) protein was detected as a loading control.

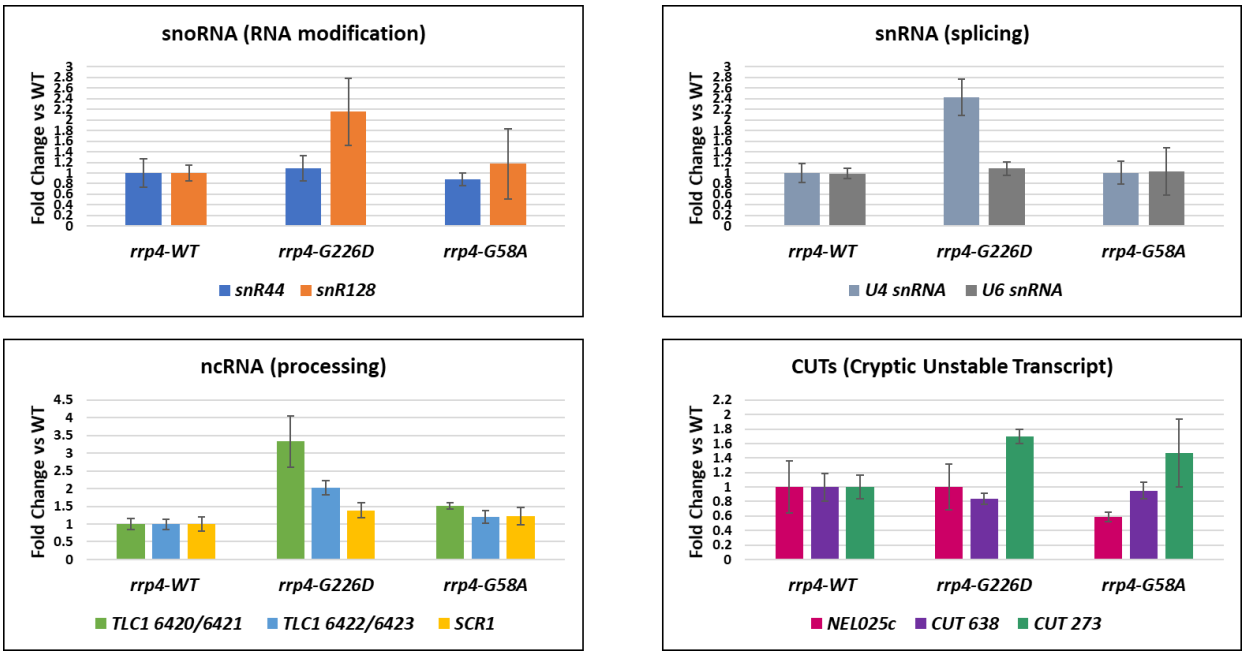


**Figure 8. Exosome RNA substrates are elevated in *rrp4-G226D* and *rrp4-G58A* mutant yeast cells.** The levels of *U4* snRNA, *TLC1* telomerase RNA, and CUT *273* ncRNA are increased in *rrp4-G226D* mutant cells, but not in *rrp4-G58A* mutant cells, relative to wildtype *RRP4* cells. RNA levels from triplicate biological samples were measured by RT-qPCR using gene-specific primers and RNA fold changes in *rrp4* mutant cells (*rrp4-G226D*, *rrp4-G58A*) relative to wildtype *RRP4* cells (*rrp4-WT*) were calculated using ΔΔCt method and graphically represented. Error bars represent standard deviation. Statistical significance was calculated using student's t-test and is denoted by asterisks (*Significant:p≤0.05; **Very significant:p≤0.01)

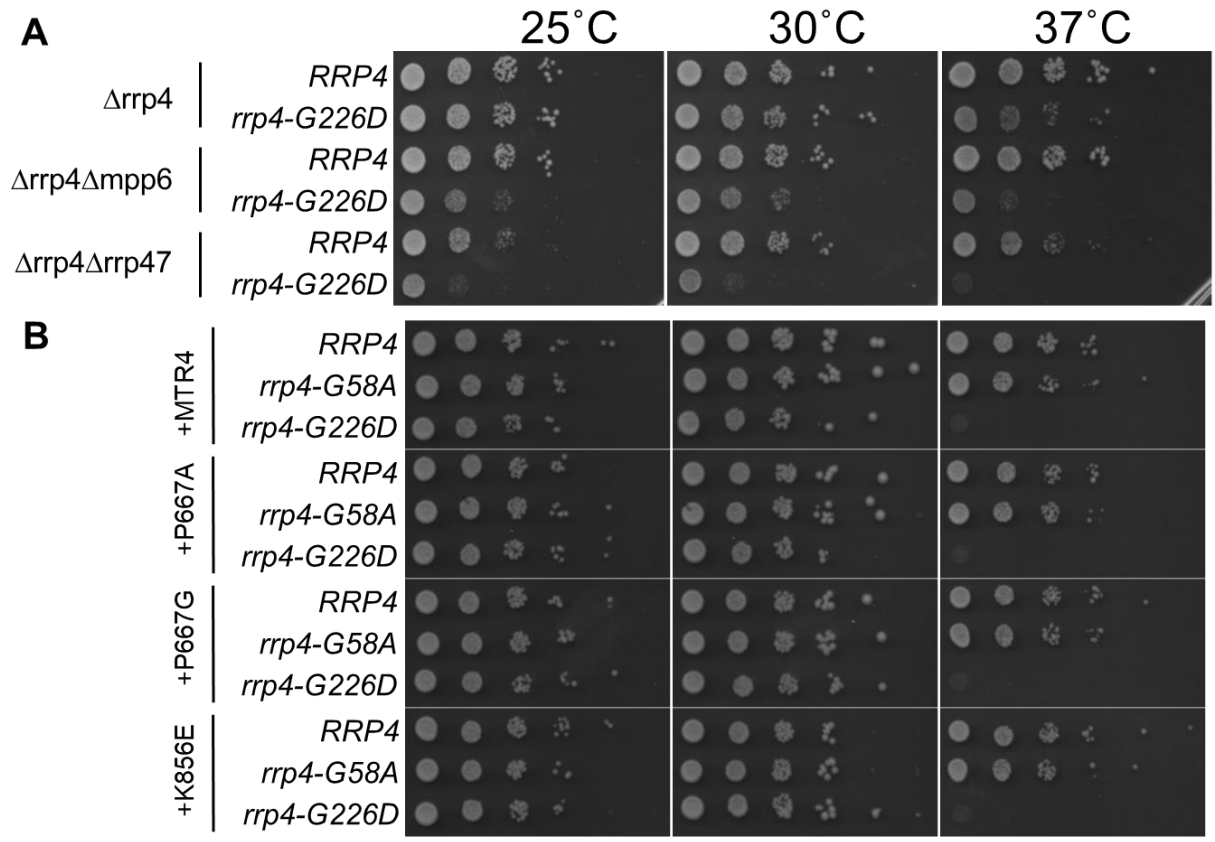


**Figure 9. The *rrp4-G226D* variant shows negative genetic interactions with *mpp6*Δ and *rrp47*Δ exosome cofactor deletion mutants, but does not exhibit genetic interactions with *mtr4* exosome cofactor missense mutants.** (A) The *rrp4-G226D mpp6*Δ and *rrp4-G226D rrp47*Δ double mutants exhibit slower growth compared to *rrp4-G226D* cells alone at all temperatures. (B) The *rrp4-G58A mtr4* and *rrp4-G226D mtr4* double mutant cells do not exhibit growth that is different compared to *rrp4-G226D* cells alone. The Δ*rrp4* Δ*mpp6*, Δ*rrp4* Δ*rrp47*, and Δ*rrp4* Δ*mtr4* cells + *mtr4* variant plasmid containing wildtype *RRP4-Myc* or *rrp4-Myc* variant plasmid as sole copy of *RRP4* were serially diluted and spotted on Leu- media and grown at indicated temperatures. The *mtr4* missense mutations tested are as follows: *mtr4-P667A, mtr4-P667G,* and *mtr4-K856E.*

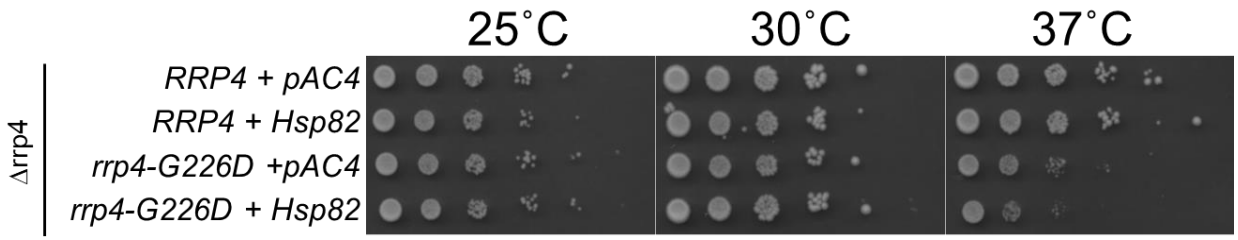


**Figure 10. Expression of Heat shock protein 82 (Hsp82) does not rescue *rrp4-G226D* growth defect.** The *rrp4*Δ cells containing wildtype *RRP4-Myc* or *rrp4-G266D-Myc* mutant test plasmid were transformed with either empty vector (pAC4) or a plasmid containing the heat shock protein 82 gene (*HSP82*) and grown on Leu- media. Plate at 25˚C plate was grown for three days and plates at 30˚C and 37˚C were grown for two days before imaging.

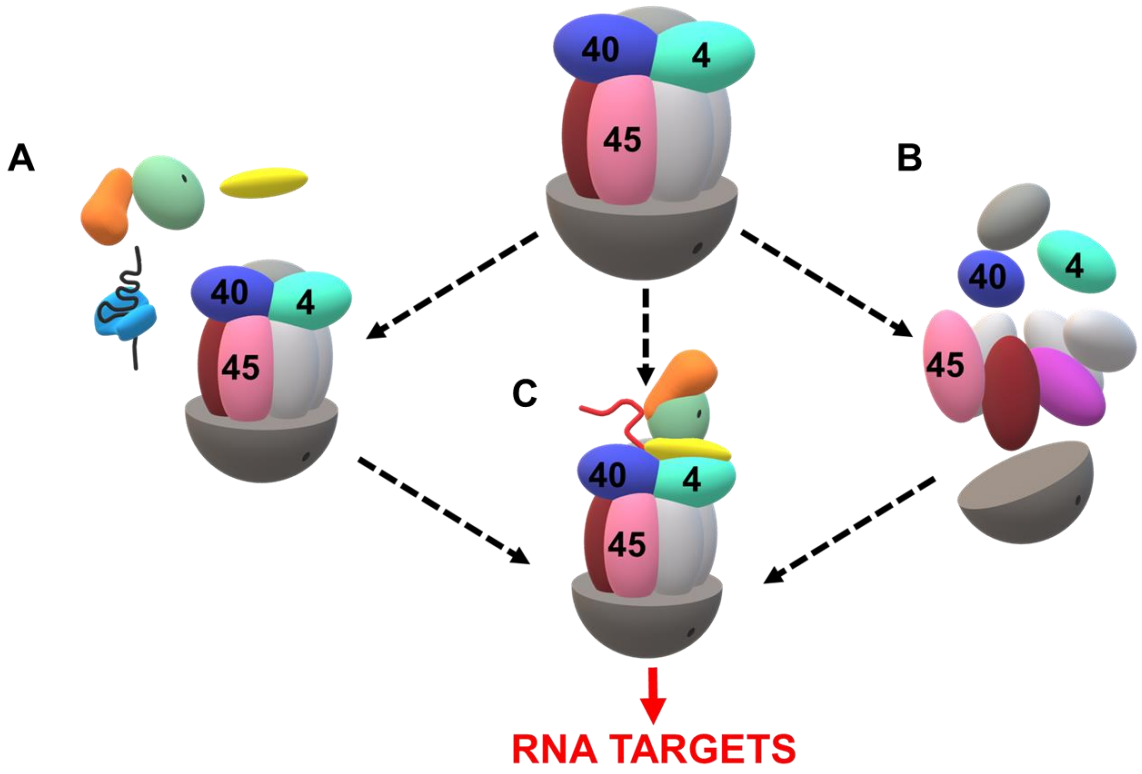


**Figure 11. Model for comparative assessment of exosomopathy mutations.** Comparing the functional consequences of *EXOSC2* mutations described in this work to the functional consequences of mutations in other RNA Exosome subunits can yield insight on the mechanism underlying patient phenotypes. Disease-linked amino acid substitutions could alter RNA exosome function by three mechanisms or a combination of the three: A) Differentially affect interactions with co-factors or the ribonuclease subunit itself. B) Differentially affects the level and stability of the subunit. This would result in changes in the assembly and disassembly of the complex. C) Affects the entry paths and interactions with specific RNA substrates. Adapted from D. J. Morton *et al.*, The RNA exosome and RNA exosome-linked disease. *RNA* **24**, 127-142 (2018).